

# Prediction of Drag Force Coefficient for Single-Column-Supported Billboard Structures

H.A.D. Samith Buddika, W.A.C. Weerasinghe and B.C.S.S.W. Rodrigo

**Abstract:** Code-based methods can only be used to determine the wind loading on single-plate billboards in the normal wind direction. No simplified methods are available to estimate the drag force coefficient for single-plate and two-plate billboards for various aspect ratios, clearance ratios and wind attack angles. Using the experimental types of research on single-plate billboards available in the literature, a database was created for the drag force coefficient, for various aspect ratios, clearance ratios and wind attack angles. In the case of two-plate billboards, a very limited number of experimental data have been reported. Hence, Computational Fluid Dynamics (CFD) Simulations were performed to investigate the variation of drag force coefficient, for various aspect ratios, clearance ratios and wind attack angles. The CFD modeling procedure was validated with the experimental results available in the literature. Two separate regression equations were developed to predict the drag force coefficients for the required aspect ratios, clearance ratios and wind angle for single-plate and two-plate billboards. The maximum torsion about the base can be estimated by multiplying the maximum drag force by 18% of the billboard width for single-plate billboards and 21% of the billboard width for two-plate billboards.

**Keywords:** Billboard, Computational fluid dynamics, Drag force coefficient, Turbulence model, Regression analysis

## 1. Introduction

Owing to increasing land prices and improvement of the road network, large single-column-supported billboard structures are becoming popular for outdoor advertising in Sri Lanka. Most of them are rectangular-shaped and 20-50m in height with reasonable clearance. These structures are often composed of steel trusses and tubes. With the height they raise above the ground, billboards are vulnerable to large wind loads. Unlike in Sri Lanka, hurricanes are frequent in some other parts of the world. That may have been the reason for the poor development of Wind Engineering in Sri Lanka. The failures of these types of structures include damage to the truss, failure of supporting structure and collapse of the whole structure resulting from foundation failure. One of the major reasons may be due to outdated and oversimplified design practices.

Wind-induced vibration, is the dynamic response of a structure due to the action of wind. This is caused by the wind-induced pressure, which is also dynamic. It is worth noting that the pressure distribution over the billboard is not uniform due to non-uniform incoming wind and the development of a boundary layer. As a result, the resulting drag force will generally be offset from the board's geometric centre. This horizontal offset

(eccentricity) results in torsion (even for the normal wind direction), which might produce significant effects on the behavior of the structure.

Wind tunnel tests to predict the wind loading on billboards are discussed in literature. While most of the studies are on single-plate billboards, only limited studies have been performed on two-plate billboards. Letchford [1] conducted wind tunnel tests for a range of rectangular signboards and hoardings with varying aspect ratios, clearance ratios and porosities for a range of wind directions. Moreover, a simplified equation to predict the drag force coefficient was also proposed, but the equation is valid only when the wind is normal to the billboard, that is when the pressure drag force becomes significant. Warnitchai et al. [2] conducted wind tunnel tests for both single-plate and two-plate

*Eng. (Dr.) H.A.D. Samith Buddika*, AMIE(SL), PhD (Tokyo Tech), M.Eng. (Tokyo Tech), B.Sc. Eng. (Peradeniya), AMSSSL, GREENAccP, Senior Lecturer, Department of Civil Engineering, Faculty of Engineering, University of Peradeniya.

Email: samithbuddia@eng.pdn.ac.lk

□ <https://orcid.org/0000-0002-4592-0738>

*Eng. W.A.C. Weerasinghe*, AMIE(SL), B.Sc. Eng. (Peradeniya)

Email: charukaweerasinghe@eng.pdn.ac.lk

□ <https://orcid.org/0000-0002-7036-9132>

*Eng. B.C.S.S.W. Rodrigo*, AMIE(SL), B.Sc. Eng. (Peradeniya)

Email: shanewrodrigo@gmail.com

□ <https://orcid.org/0000-0001-7800-5133>



billboards and presented the variation of drag force coefficient and eccentricity with wind direction. Zuo et al. [3] conducted a three-phase experimental campaign to study wind loading on rectangular box type, single-plate and two-plate sign structures. Li et al. [4] conducted wind tunnel experiments to investigate the wind loading on two-plate billboards.

Full-scale field tests on billboards also have been performed by Smith et al. [5].

Results obtained from wind tunnel testing have helped in developing wind load standards to guide the designing of structures for wind loading (AS/NZS 1170.2 [6], Eurocode 1-1-4 [7], ACSE/SEI 7 [8]). However, code-based methods cannot be used to design of billboards for required aspect ratios, clearance ratios and wind angles.

In the present study, two regression equations were developed to predict the drag force coefficients for the required aspect ratios, clearance ratios and wind angle for single-plate and two-plate billboards. Moreover, a simplified method to predict the maximum torsion about the base of the billboards is also proposed.

## 2. Review of Code-based Methods to Calculate the Wind Forces on Billboards

In this study, AS/NZS 1170.2 [6], Eurocode 1-1-4 [7], and ACSE/SEI 7 [8] codes of practice were examined to understand the analytical procedure to predict the drag force acting on a billboard.

All three codes of practice showed similarities in their approach to determine the design drag force acting on a billboard. The design codes consider the terrain and the exposure level of the structure, but the design codes provide factors that are compatible with their countries and may not be suitable in the Sri Lankan context. The design codes also do not consider the wind attack angle specifically, therefore unable to predict the drag force that acts when the wind is not flowing perpendicular to the billboard. In addition, the design codes do not provide any procedure to design the drag force acting on two-plate billboards.

### 2.1 Australia/New Zealand Standard

According to the AS/NZS 1170.2 [6], initially the site wind speed is determined followed by the design wind speed, before the wind

pressure is calculated, and finally the wind action is calculated. The following equation is used to determine the site wind speed ( $V_{sit,\beta}$ );

$$V_{sit,\beta} = V_R M_d (M_{z,cat} M_s M_t) \quad \dots(1)$$

Where,  $V_R$  is the regional gust wind speed in meters per second.  $M_d$ ,  $M_{z,cat}$ ,  $M_s$  and  $M_t$  are wind directional multiplier, terrain/height multiplier, shielding multiplier and the topographic multiplier respectively. After determining  $V_{sit,\beta}$ , the design wind speed is taken as the maximum cardinal direction site wind speed. Thereafter the following equation is used to determine the design wind pressure:

$$p = (0.5 \rho_{air}) [V_{des,\theta}]^2 C_{fig} C_{dyn} \quad \dots(2)$$

where,  $\rho_{air}$  is the density of air,  $1.2 \text{ kg/m}^3$ ,  $V_{des,\theta}$  is the design wind speed,  $C_{fig}$  is the aerodynamic shape factor and  $C_{dyn}$  is the dynamic response factor. Finally, design wind force is calculated by multiplying the design wind pressure by the area of the billboard.

### 2.2 European Standard

When considering the Eurocode 1-1-4 [7], after determining the respective terrain category for the structure, mean wind velocity,  $V_m$  at the reference height is determined using the following equation:

$$V_m(z) = C_r(z) C_o(z) V_b \quad \dots(3)$$

Where,  $C_r(z)$ ,  $C_o(z)$  and  $V_b$  are roughness factor, orography factor and basic wind velocity respectively. Next, the Turbulence Intensity,  $I_v$  is calculated using the following equation:

$$I_v(z) = k_l / [C_o(z) \cdot \ln(z/z_0)] \quad \dots(4)$$

Where,  $k_l$  is the turbulence factor and  $z_0$  is the the roughness length respective to the terrain category. Thereafter peak velocity pressure,  $q_p$  is calculated from the equation below:

$$q_p(z) = (1 + 7 \cdot I_v(z)) \cdot (1/2) \cdot \rho \cdot v_m(z)^2 \quad \dots(5)$$

Finally, the wind force acting on the billboard is calculated by multiplying the peak velocity pressure by the area of the billboard.

### 2.3 ASCE Standard

According to the ACSE/SEI 7 [8], initially the category corresponding to the structure and the exposure class should be determined. Then the velocity pressure,  $q_z$  is computed using the following equation:

$$q_z = 0.00256 K_z K_{zt} K_d V^2 psf \quad \dots(6)$$

where,  $V$  is the basic wind speed,  $K_{zt}$  is the topographic factor,  $K_d$  is the wind

directionality factor and  $K_z$  is the velocity pressure exposure coefficient [9]. Thereafter, design force ( $F$ ) acting on the structure is calculated from the following equation:

$$F = q_z G C_f A_s \quad \dots (7)$$

Where,  $G$  is the gust effect factor,  $C_f$  is the force coefficient and  $A_s$  is the gross area of the solid sign.

### 3. Evaluation of Drag Force Coefficient using Measured Forces

#### 3.1 Mean Drag Force Coefficient for Single-Plate Billboards

A billboard model fixed on a multi-component force sensor is shown in Figure 1. The sensor can measure six force components. It is worth to note that, only two of the force components are truly relevant for the structural design of a billboard: drag force  $F_x$  and the torsional moment around the centre axis of supporting column,  $M_z$ . The other components are relatively small and can be neglected. For single-plate billboards, the mean drag force coefficient,  $C_D$  is given by the following expression (Warnitchai et al. [2]):

$$C_D = \frac{\bar{F}_x}{\frac{1}{2}\rho\bar{U}^2bd} \quad \dots (8)$$

Where,  $\bar{F}_x$  is the mean value of the force component normal to the board. The wind loading on a billboard is highly dependent on its geometry and the wind attack angle ( $\theta$ ). Since most of the billboards are rectangular, the geometry can be defined in terms of aspect ratio ( $b/d$ ) and clearance ratio ( $d/h$ ) (Figure 2).  $\bar{U}$  is the mean wind velocity which is set to 45 km/h for this study.

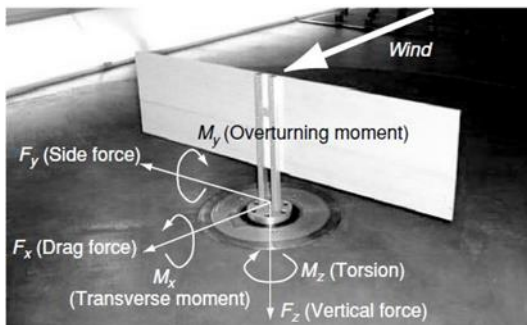


Figure 1 - A Billboard Model Fixed on a Multi-Component Force Sensor by Warnitchai et al. [2]

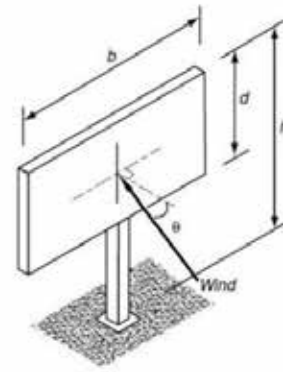


Figure 2 - Model Geometry of a Single-Panel Billboard (Warnitchai et al. [2])

#### 3.2 Total Force Coefficient for Two-Plate Billboards

To define the wind loading on two-plate billboards, a reference plane is introduced between the two plates such that it bisects the angle ( $\phi$ ) between them as shown in Figure 3 (Warnitchai et al. [2]).

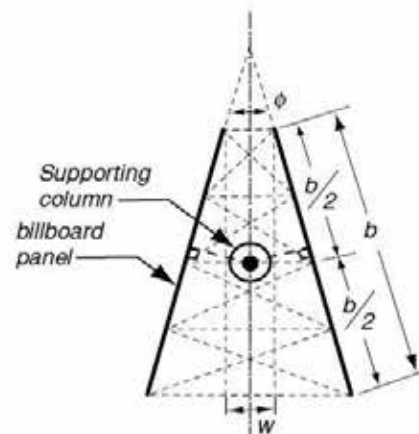


Figure 3 - Plan view of the Model Geometry showing the Reference Plane for Two-Plate Billboards (Warnitchai et al. [2])

Apart from the normal force/drag force  $F_x$ , the side force  $F_y$ , is also significant in most cases. Therefore, instead of the drag force coefficient, the total force coefficient,  $C_{F_t}$  is used.  $F_t$  denotes the total force acting on the billboard (Warnitchai et al. [2]).

$$\bar{F}_t = \sqrt{\bar{F}_x^2 + \bar{F}_y^2} \quad \dots (9)$$

$$C_{F_t} = \frac{\bar{F}_t}{\frac{1}{2}\rho\bar{U}^2bd} \quad \dots (10)$$

#### 3.3 Torsional Moment about the Column Base of Billboard

The torsion can be considered as the drag force acting at a horizontal eccentricity ( $e$ ) from the



geometric centre of the board. Based on the results obtained in the present study, simplified methods to calculate the torsional moment about the column base of billboards were introduced for both single-plate and two-plate billboards.

#### 4. Computational Fluid Dynamics Simulations

Computational fluid dynamics (CFD) offers a very powerful alternative to predict the wind-related phenomena on structures. Midas NFX software package was used for this purpose in the present study. Simulations were carried out considering the same parameters used for wind tunnel testing of billboards. The simulation procedure was validated by comparing with the experimental results available in the literature.

##### 4.1 Navier-Stokes Equations

Wind flow around bluff bodies is governed by incompressible Navier-Stokes Equation (11) and the Continuity Equation (12).

$$\frac{\partial \rho}{\partial t} + \frac{\partial(\rho u_i)}{\partial x_i} = 0 \quad \dots (11)$$

$$\frac{\partial(\rho u_i)}{\partial t} + \frac{\partial(\rho u_i u_j)}{\partial x_j} = -\frac{\partial P}{\partial x_i} + \frac{\partial}{\partial x_j} \left( \mu \left( \frac{\partial u_i}{\partial x_j} + \frac{\partial u_j}{\partial x_i} \right) \right) \quad (12)$$

where,  $u_i$ ,  $u_j$ ,  $\rho$ ,  $P$ ,  $\mu$ , and  $t$  are velocity components, air density, air pressure, dynamic viscosity and time respectively. In these equations, Coriolis force and buoyance force are not included as their effect is negligible for micro-scale CFD simulations. In Direct Numerical Simulation (DNS), these equations are directly solved which require very fine grids to capture all relevant scales in the flow. As its computational demand is too high for the Reynolds numbers typically encountered in wind engineering, it is not applicable in this area. The generally used approach for the computation of turbulent flows in wind engineering is the Reynolds Averaged Navier-Stokes equations (RANS). In this approach, the equations are averaged in time over all the turbulent scales to obtain a statistically steady solution of flow variables. So, any variable in a turbulent flow can be represented as a sum of mean value and a fluctuating value.

$$u_j = U_j + u'_j \quad \dots (13)$$

Where,  $U_j$  is the mean velocity and  $u'_j$  is the fluctuating component in a turbulent flow. Substituting Equation (13) in Equation (12)

using the fact that mean value of the fluctuating component,  $\overline{u'_j} = 0$ ,

$$\frac{\partial(\rho U_i)}{\partial t} + \frac{\partial \rho (U_i U_j + \overline{u'_i u'_j})}{\partial x_j} = -\frac{\partial \overline{P}}{\partial x_i} + \frac{\partial}{\partial x_j} \left( \mu \left( \frac{\partial U_i}{\partial x_j} + \frac{\partial U_j}{\partial x_i} \right) - \rho \overline{u'_i u'_j} \right) \dots (14)$$

The extra fluctuating term,  $\rho \overline{u'_i u'_j}$  is known as Reynolds stress. A turbulence model is used to represent this in terms of mean quantities.

##### 4.2 k- $\omega$ SST Turbulence Model

The Shear-Stress Transport (SST) model was developed recently for accurate prediction of aeronautic flows with adverse pressure gradients and separation (Murakami [11] and Menter et al. [12]). Over decades, the existing models have consistently failed to compute these flows accurately. In particular, the otherwise popular k- $\epsilon$  model was not able to predict the behavior of boundary layers up to the separation. The k- $\omega$  model is substantially more accurate than k- $\epsilon$  in the near-wall regions. It calculates two convective transport equations for specific dissipation rate of turbulent kinetic energy ( $\omega$ ) and turbulent kinetic energy ( $k$ )

$$k = \frac{1}{2} (\overline{u^2} + \overline{v^2} + \overline{w^2}) \quad \dots (15)$$

Where,  $u$ ,  $v$ ,  $w$  are wind velocity components, along lateral and vertical directions. To calculate accurate values of the turbulence, the eddy kinetic energy and eddy length scale need to be defined according to the following equations;

$$\text{Eddy kinetic energy} = 1.5 \times (\text{velocity} \times \text{turbulence intensity level})^2 \quad \dots (16)$$

$$\text{Eddy length scale} = \frac{10 \times \text{viscosity}}{(\rho \sqrt{\text{Eddy kinetic energy}})} \quad \dots (17)$$

The Reynolds number of the flow was set to  $1 \times 10^5$ . The degree of accuracy of these components directly affects the accuracy of the simulation.

##### 4.3 Computational Domain and Boundary Conditions

The computational domain is dependent on the size of the model billboard. However, the domain should be large enough to avoid the interference of the boundary with the flow. As the thickness of the billboard is not significant, the domain was selected based on the height and width (Figure 4).

The boundary conditions represent the influence of the surrounding that has been separated by the computational domain. Boundary conditions incorporated for this study is depicted in Figure 5.

Inlet condition corresponding to the wind velocity is applied on the front face. Outflow is at atmospheric pressure. Hence, 0 Pa was applied on the rear face. CFD analysis is the analysis of liquid or gas flow, thus solid parts are not directly considered in the analysis and wall condition should be used on faces that are in contact with solid parts and no-slip condition was applied on the walls. To represent the fact that the air around is almost infinitely large, the normal velocity=0 condition was applied to the faces at the boundary with the atmosphere.

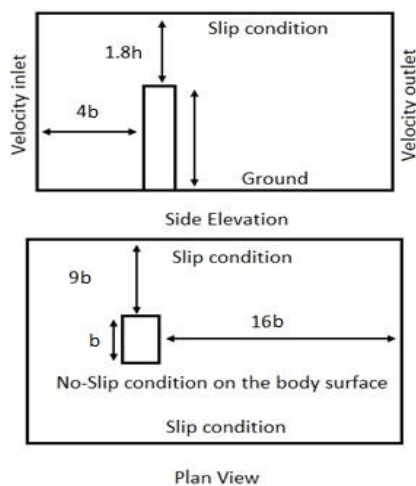


Figure 4 - Computational Domain Size Used in the Present Study (Deraman et al. [10])

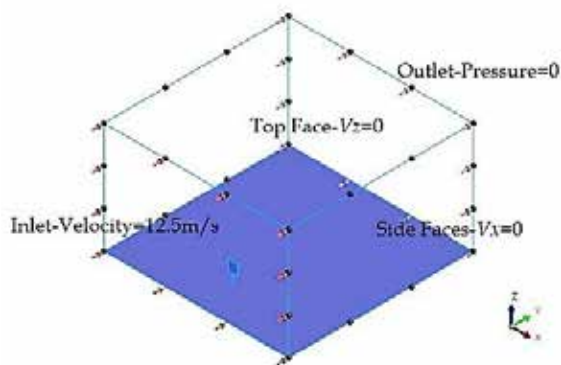


Figure 5 - Boundary Conditions of the Domain

#### 4.4 Mesh Generation

The accuracy of CFD results highly depend on the mesh being used. Both triangle and quadrilateral elements (hybrid) were used in the mesh generation (Weerasuriya [13]). The

nodal displacement variation of the billboard corresponding to  $\theta=0$  is depicted in Figure 6. As expected, the largest lateral deformation was observed at the top of the billboard. The most fundamental and accurate method for evaluating mesh quality is to refine the mesh until the results converge to a particular value, which is known as a mesh sensitivity analysis. For each model, a sensitivity analysis was carried out. For the case of clearance ratio=0.33 and aspect ratio=1, the sensitivity analysis results are shown in Table 1. It can be seen that, although the number of elements increase, the result remains constant (converged) around 1.29. As a mesh quality check, the aspect ratio was assured to be less than 3 for over 95% of the elements generated in the mesh.

Table 1 - Mesh Sensitivity Analysis Results for Billboard with Aspect Ratio =1, Clearance Ratio =0.33

Edge size control (mm)	No. of elements	Drag force coefficient
2.75	984676	1.323
2.40	992468	1.297
2.00	1039590	1.304
1.90	1041899	1.291
1.80	1054653	1.296

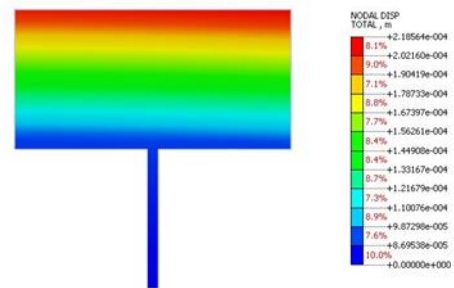


Figure 6 - Variation of Nodal Displacement of the Billboard Corresponding to  $\theta=0$

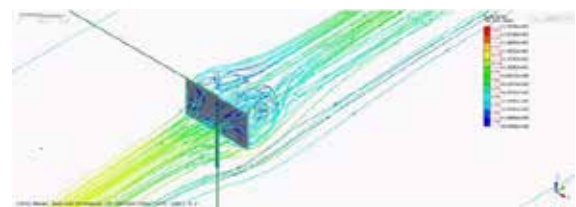


Figure 7 - Fluid Flow around a Billboard corresponding to  $\theta=0$

#### 4.5 Validation of Computational Fluid Dynamics Simulation Procedure

The CFD simulation procedure was validated by comparing with the results of wind tunnel tests of billboards using high-frequency force balance (HFFB) technique given in Warnitchai



et al. [2]. The material of the billboard was balsa wood with unit mass ( $\rho$ ) =  $150\text{kg/m}^3$  and Young's modulus ( $E$ ) =  $3.71\text{GPa}$ . The density of air was taken as  $1.225\text{ kg/m}^3$ . In the case of single-plate billboards, 9 scaled models of rectangular billboards with aspect ratio  $b/d$  of 1, 2, and 3 and clearance ratio  $d/h$  of 0.33, 0.50, and 0.67 were tested. This test series was intended to cover various possible configurations of single-panel billboards in Thailand. The geometric scaling ratio was set to 1:200. All models in the first series were 25 cm high, which corresponds to 50 m in the full scale. Fluid flow around a billboard

corresponding to  $\theta=0^\circ$  is depicted in Figure 7, for a single-plate billboard. All models were tested for wind attack angles  $0^\circ, 15^\circ, 30^\circ, 45^\circ, 60^\circ$  and  $75^\circ$ . Typical fluid pressure distribution for different wind attack angles are shown in Figure 8. Figure A1 in Annex A shows the comparison between CFD results and experimental results for single-plate billboards. Results obtained from CFD simulations showed good agreement with the HFBB results for single-plate billboards.

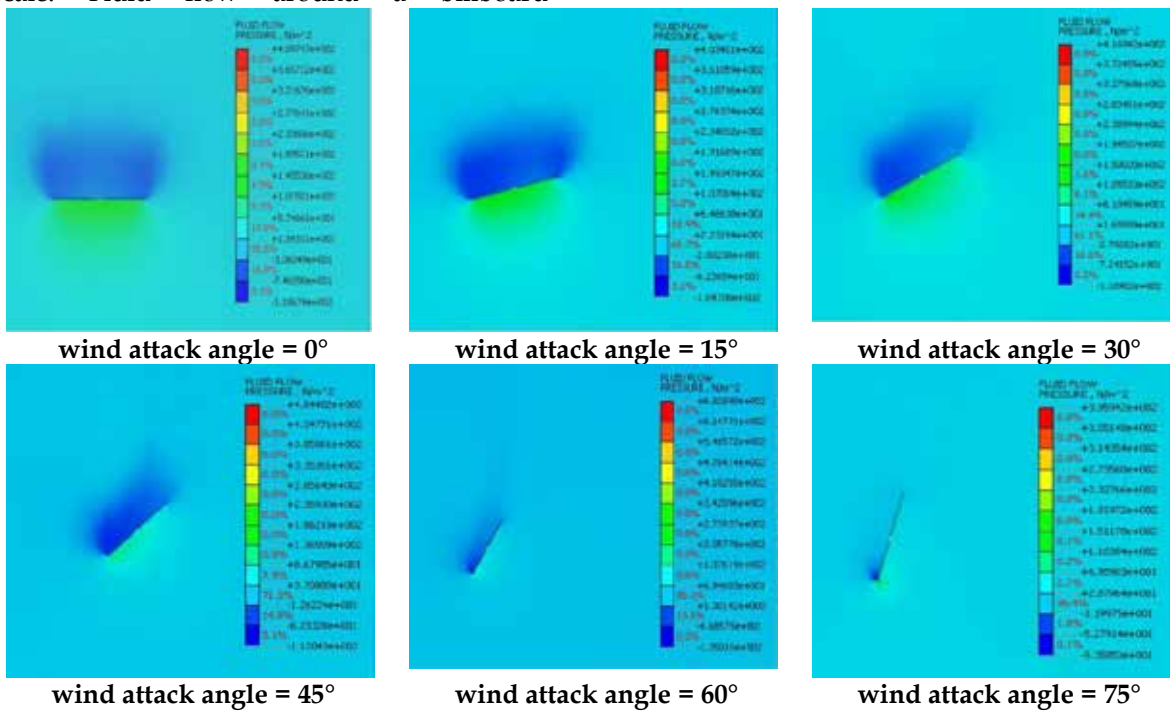


Figure 8 - Typical Fluid Pressure Distribution for Wind Attack Angles  $0^\circ, 15^\circ, 30^\circ, 45^\circ, 60^\circ, 75^\circ$

In the case of two-plate billboards, limited test results are available from past studies. Two-plate billboard with aspect ratio 2 and clearance ratio 0.5 with angle between plates ( $\phi$ )  $0^\circ, 15^\circ, 30^\circ$  was tested. The lessons learnt during the simulation of single-plate billboards were adopted during the simulation of two-plate billboards. Figure A2 in Annex A shows the comparison between CFD results and HFBB results for two-plate billboards. Results obtained from CFD simulations showed good agreement with the experimental results for two-plate billboards. The validated CFD simulation procedure was used to generate a database of the variation of drag force coefficient, with various aspect ratios, clearance ratios and wind attack angles for two-plate billboards.

## 5. Equations to Calculate the Drag Force Coefficients and Peak Eccentricity Ratio

### 5.1 Single-Plate Billboards

#### 5.1.1 Equation to Calculate the Drag Force Coefficient for Single-Plate Billboards

Using the experimental results on single-plate billboards available in the literature, a database was created for the drag force coefficient, for various aspect ratios, clearance ratios and wind attack angles. The database consisted of 139 results. RStudio package was used for the regression analysis.

First, a linear regression was carried out treating first-order terms of aspect ratio, clearance ratio and wind attack angle as predictor variables and drag coefficient as the

predicted variable. The adjusted R2 value obtained using linear regression was 0.685. Since R2 value alone doesn't provide a complete understanding regarding the accuracy of the regression equation, the proposed equation was compared with experimental data and the drag force coefficient calculated using linear regression did not agree well with the experimental results. Therefore multivariable regression model with higher order terms are proposed as shown in Equation (18). The R<sup>2</sup> value was found to be 0.827.

$$C_D = -0.364 - 0.13 \log_{10} AR - 0.308(CR)^3 + 4.138 \cos(\theta) - 2.315 \cos^2 \theta \quad \dots (18)$$

The drag force coefficient calculated using Equation 18 agreed well with the experimental results and the validation using aspect ratio=2, clearance ratio=0.5 is shown in Figure 9.

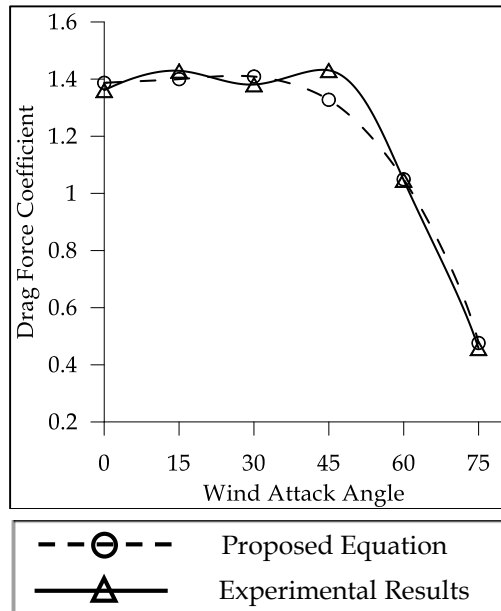


Figure 9 - Validation of the Proposed Equation for Single-plate billboards

### 5.1.2 Method to Calculate Peak Eccentricity Ratio for Single-plate Billboards

In order to develop a simplified method to calculate the maximum torsional moment about the base of single-plate billboards, the peak eccentricity ratio,  $e_p/b$  versus wind angle was plotted. For this purpose, results from nine scaled models of rectangular billboards with aspect ratio  $b/d$  of 1, 2, and 3 and clearance ratio  $d/h$  of 0.33, 0.50, and 0.67 used during the validation procedure were used. The variation of peak eccentricity ratio,  $e_p/b$  with wind angle is shown in Figure 11. Based on the results shown in Figure 11, a value of 0.18 can be recommended as a conservative value for  $e_p/b$ . Therefore, a conservative value

for torsional moment can simply be calculated by multiplying the drag force by 0.18b.

## 5.2 Two-Plate Billboards

### 5.2.1 Equation to calculate the Drag Force Coefficient for Two-plate Billboards

Experimental results on two-plate billboards are very limited. Hence to develop a database for two-plate billboards, CFD simulations were carried out for various aspect ratios, clearance ratios and angle between the plates such that they represent possible configurations of two-plate billboards. Simulations were carried out for wind attack angle  $\theta$  of 0°, 15°, 30°, 45°, 60°, 75° and 90°. For each wind attack angle the angle between two plates,  $\phi$ , varied from 0°, 15° and 30°. The database for two-plate billboards consisted of 105 results.

An expression for the total force coefficient is presented in terms of aspect ratios, clearance ratio, wind attack angle and the angle between the plates. Two separate expressions were formulated for  $\theta$  from 0-45° and 45°-90°.

$$0 < \theta < 45^\circ$$

$$C_{Ft} = 1.787 - 0.041AR - 0.228CR - 1.246 \cos \phi + 1.214 \cos \theta \quad \dots (19)$$

$$45^\circ < \theta < 90^\circ$$

$$C_{Ft} = 2.514 - 0.103AR - 0.389CR - 1.881 \cos \phi + 1.4 \cos \theta \quad \dots (20)$$

The drag force coefficient calculated using Equations (19) and (20) follow the similar trend as experimental results (Figure A2 (a)) and the variation is shown in Figure 10.

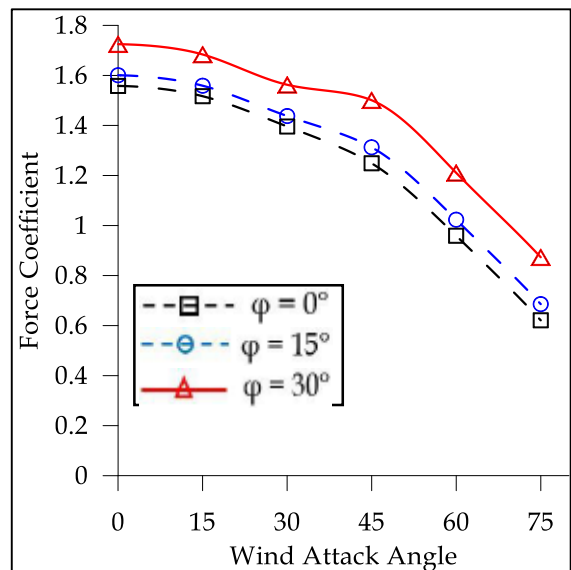


Figure 10 - Validation of the Proposed Equation for Two-plate billboards



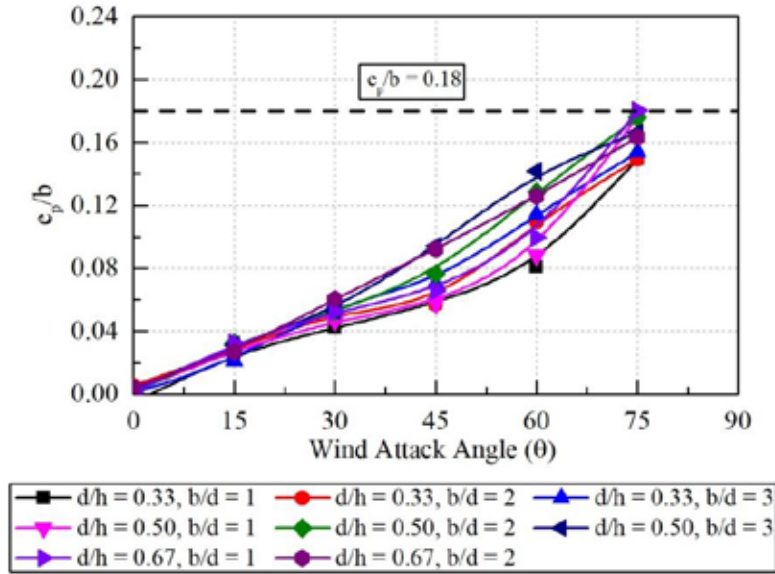


Figure 11 - Variation of Peak Horizontal Eccentricity Ratio with Wind Attack Angle for Single-Plate Billboards

5.2.2 Method to Calculate Peak Eccentricity Ratio for Two-Plate Billboards

Figure 12 shows the variation of  $e_p/b$  against wind attack angle for various configurations. The behavior of  $\phi=0^\circ$  case is identical to that of single-plate billboards. Hence, torsional response of parallel two-plate billboards can be estimated by multiplying the total force by

0.18b, as similar to single-plate billboards. For both  $\phi=15^\circ$  and  $\phi=30^\circ$  cases, maximum  $e_p/b$  is identified as 0.21. Therefore, torsional response of non-parallel two-plate billboards can be estimated by multiplying the total force by 0.21b.

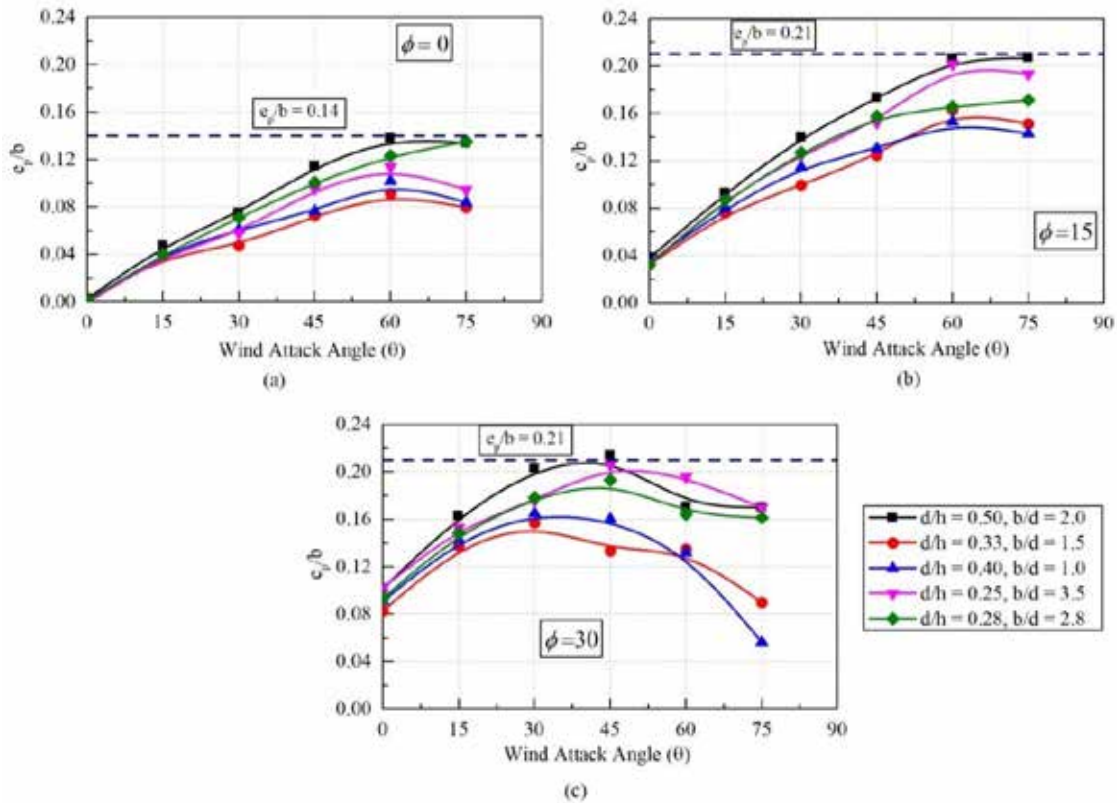


Figure 12 - Variation of Peak Eccentricity Ratio with Wind Angle for Two-Panel Billboards



## 6. Summary and Conclusions

Numerous wind tunnel experiments have been carried out to investigate the wind loading on single-plate billboards in the literature. A database was formed using the tabulated data available in the literature for further analysis.

Unlike single-plate billboards, limited research has been carried out on two-plate billboards. To generate adequate data and to form a database, CFD analyses were done. Out of the different turbulence models available,  $k-\omega$  SST model overcomes almost all the shortcomings in predicting the wind loads on billboards.

Using the databases generated for single-plate and two-plate billboards, two separate equations were formulated to easily predict the drag force coefficient and hence the drag force. With the results obtained, the following conclusions can be made:

1. Code-based approaches can only be used to determine wind forces for normal wind direction and they do not provide any provision for two-plate billboards.
2.  $k-\omega$  SST turbulence model serves better for simulation of billboards.
3. Proposed Equation (18) can be employed to predict the drag force coefficient for single-plate billboards during the design.
4. Proposed Equations (19) and (20) can be employed to predict the total force coefficient for two-plate billboards during the design.
5. Torsional response of single-plate billboards and parallel-plate billboards can be estimated by multiplying the drag force by 0.18b.
6. Torsional response of non-parallel two-plate billboards can be estimated by multiplying the total force by 0.21b.

## References

1. Letchford, C. W. "Wind Loads on Rectangular Signboards and Hoardings." *Journal of Wind Engineering and Industrial Aerodynamics* 89, no. 2 (2001): 135-151.
2. Warnitchai, P., Suksit S., and Kobchai P. "Wind Tunnel Model Tests of Large Billboards." *Advances in Structural Engineering* 12, No. 1 (2009): 103-114.
3. Zuo, D, Douglas A. S., and Kishor C. M. "Experimental Study of Wind Loading of Rectangular Sign Structures." *Journal of Wind Engineering and Industrial Aerodynamics* 130 (2014): 62-74.
4. Li, Z., Dahai W., Xinzhong C., Shuguo L., and Jie L. "Wind Load Effect of Single-Column-Supported Two-Plate Billboard Structures." *Journal of Wind Engineering and Industrial Aerodynamics* 179 (2018): 70-79.
5. Douglas A. S., Delong Z., and Kishor C. M. "Characteristics of Wind Induced Net Force and Torque on a Rectangular Sign Measured in the Field." *Journal of Wind Engineering and Industrial Aerodynamics* 133 (2014): 80-91.
6. Australian and New Zealand standards: Structural Design Actions Part 2: Wind actions; AS/NZS 1170.2:2002
7. Eurocode 1: Actions on structures – Part 1-4: General actions – wind actions. EN 1991-1-4:2005
8. American Society of Civil Engineers (ASCE). *Minimum Design Loads for Buildings and other Structures*. Reston (VA): ASCE/SEI 7; 2010.
9. Cook, N J. "The Designer's Guide to Wind Loading of Building Structures. Vol. 2: Static Structures." *Building Research Establishment Report* (1990).
10. Deraman, S. N. C., Majid, T. A., Zaini, S. S., Yahya, W. N. W., Abdullah, J., and Ismail, M. A. "Enhancement of CFD Validation Exercise along the Roof Profile of a Low-Rise Building." *IOP Conference Series: Earth and Environmental Science*, Vol. 140, No. 1, p. 012004. IOP Publishing, 2018.
11. Murakami, S. "Computational Wind Engineering." *Journal of Wind Engineering and Industrial Aerodynamics* 36 (1990): 517-538.
12. Menter, F. R., Kuntz, M., and Langtry, R. "Ten Years of Industrial Experience with the SST Turbulence Model." *Turbulence, heat and mass transfer* 4, No. 1 (2003): 625-632.
13. Weerasuriya, A. U. "Computational Fluid Dynamic (CFD) Simulation of Flow around Tall Buildings." *Engineer: Journal of the Institution of Engineers, Sri Lanka* 46, No. 3 (2013).



## Annex A- Comparison of CFD Simulation Results with HFBB Results

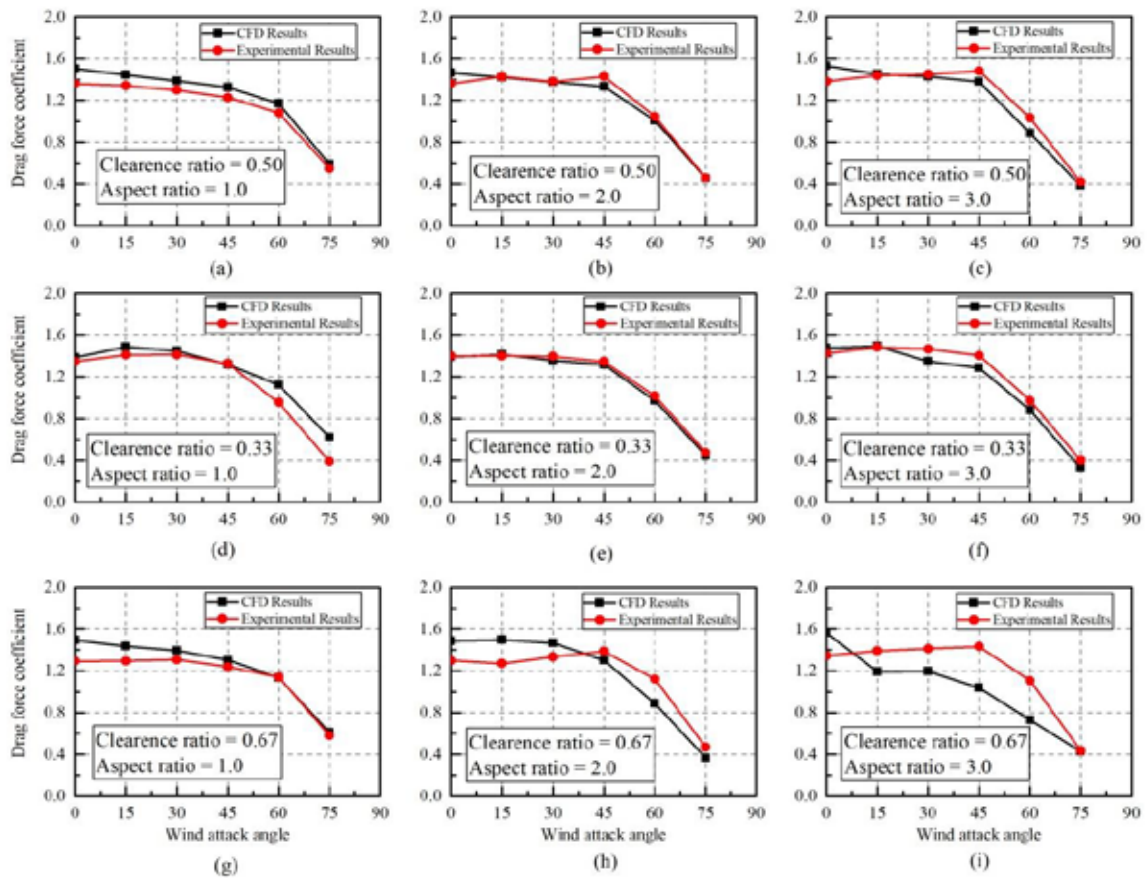
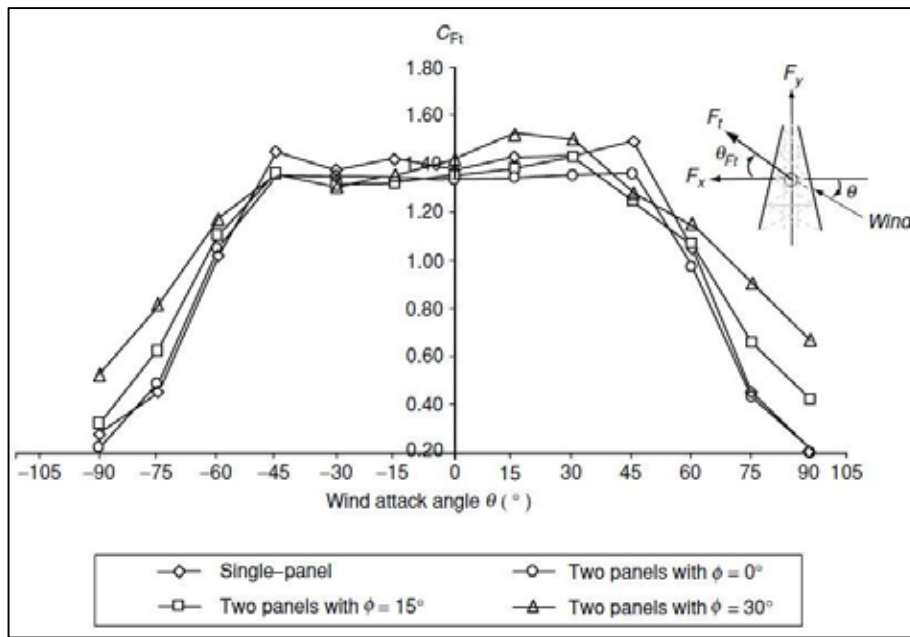
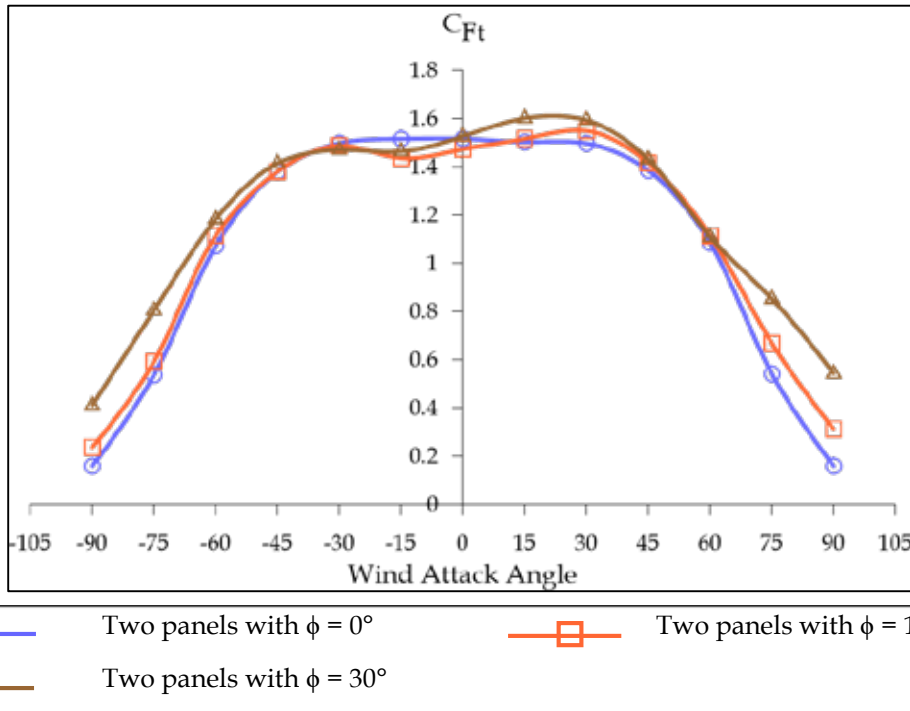


Figure A1 - Comparison of CFD Simulation Results with HFBB Results for Single-plate Billboards reported in Warnitchai et al. [2]: (a)-(c) clearance ratio is 0.33; (d)-(f) clearance ratio is 0.5; (g)-(i) clearance ratio is 0.67



(a) HFBB results for two-plate billboards reported in Warnitchai et al. [2].



(b) CFD Simulation Results

Figure A2 - Comparison of CFD Simulation Results with HFBB Results for Two-plate Billboards reported in Warnitchai et al. [2]: (a) HFBB Results for Two-plate Billboards; (b) CFD Simulation results

